

Cite this: DOI: 10.1039/c2an16210e

www.rsc.org/analyst

PAPER

A novel sensor of cysteine self-assembled monolayers over gold nanoparticles for the selective determination of epinephrine in presence of sodium dodecyl sulfate†

Nada F. Atta,* Ahmed Galal* and Ekram H. El-Ads

Received 5th December 2011, Accepted 20th March 2012

DOI: 10.1039/c2an16210e

A novel sensor of cysteine self-assembled monolayers over gold nanoparticles modified gold electrode has been constructed for the determination of epinephrine in presence of sodium dodecyl sulfate (Au/Au_{nano}-Cys⋯SDS). Electrochemical investigation and characterization of the modified electrode are achieved using cyclic voltammetry, linear sweep voltammetry, and scanning electron microscopy. The Au/Au_{nano}-Cys⋯SDS electrode current signal is remarkably stable *via* repeated cycles and long term stability, due to the strong Au–S bond, compared to the Au/Au_{nano} electrode. The catalytic oxidation peak currents obtained from linear sweep voltammetry (LSV) increased linearly with increasing epinephrine concentrations in the range of 2 to 30 μmol L⁻¹ and 35 to 200 μmol L⁻¹ with correlation coefficients of 0.9981 and 0.9999 and a limit of detection of 0.294 nmol L⁻¹ and 1.49 nmol L⁻¹, respectively. The results showed that Au/Au_{nano}-Cys⋯SDS can selectively determine epinephrine in the coexistence of a large amount of uric acid and glucose. In addition, a highly selective and simultaneous determination of tertiary mixture of ascorbic acid, epinephrine, and acetaminophen is explored at this modified electrode. Excellent recovery results were obtained for determination of epinephrine in spiked urine samples at the modified electrode. Au/Au_{nano}-Cys⋯SDS can be used as a sensor with excellent reproducibility, sensitivity, and long term stability.

1. Introduction

Epinephrine (EP), a hormone secreted by the medulla of adrenal glands,¹ is an important catecholamine neurotransmitter in the mammalian hormonal² and central nervous system. Epinephrine, which exists in the nervous tissue and body fluids as large organic cations,^{3,4} belongs to the family of inhibitory neurotransmitters which are used for the message transfer in biology.^{5,6} Presence of epinephrine in the body affects the regulation of blood pressure and the heart rate, lipolysis, immune system, and glycogen metabolism.⁷ It also serves as a chemical mediator for conveying the nerve pulse to efferent organs.^{1,3} Low levels of epinephrine have been found in patients with Parkinson's disease.⁵ When epinephrine is secreted into the bloodstream, it rapidly prepares the body for action in an emergency.⁸ Medically, it is a drug which has been used as a common emergency healthcare medicine^{3,8} for emergency treatment in severe allergic reaction, cardiac arrest and sepsis.⁷ Therefore, the quantitative determination of epinephrine concentration in different human fluids,⁵

such as plasma and urine, is important for developing nerve physiology, pharmacological research and life science.^{4,7}

Various modified electrodes^{9–13} have been constructed to be used as electrochemical sensors for epinephrine such as Pd nanoclusters modified poly(3-methylthiophene) (PMT), and poly(*N*-methylpyrrole) (PMPy) film-coated platinum (Pt) electrode,^{14–16} poly(3,4-ethylene dioxythiophene) modified platinum electrode in the presence of sodium dodecyl sulfate (SDS),¹⁷ carbon paste electrode modified with gold nanoparticles¹⁸ or iron(II) phthalocyanine,³ gold nanoclusters deposited on ultrathin overoxidized polypyrrole (PPyox) film modified glassy carbon electrode,¹⁹ multi-walled carbon nanotube modified with cobalt phthalocyanine in a paraffin composite electrode,²⁰ self-assembled monolayer (SAM),^{1,21,22} and gold nanoparticles immobilized on SAM modified electrodes.^{2,23}

The self-assembly procedure is a precise modification of the surface structure on a nanometer-scale, which has been employed recently in the fabrication of sensors and biosensors.²⁴ In particular the self-assembly of organosulfur compounds on gold surface have been extensively studied.^{25–31} It has been shown that organosulfur compounds upon spontaneous chemisorption on gold surface, lose the hydrogen from the thiol group as molecular hydrogen H₂ and a strong, covalent and thermodynamically favored S–Au bond is formed.^{32,33} The reason for adsorbing thiols on gold as a preferred substrate is based on two

Department of Chemistry, Faculty of Science, Cairo University, 12613 Giza, Egypt. E-mail: nada_fahl@yahoo.com; galal@sci.cu.edu.eg; Fax: +20 235727556; Tel: +20 237825266

† Electronic supplementary information (ESI) available. See DOI: 10.1039/c2an16210e

considerations: first, gold is a relatively inert metal and does not form stable oxides on its surface, second, it has a strong specific interaction with sulfur, which allows the formation of stable monolayers³² in a very reproducible way³⁴ and in a short time.³⁵ The stable, well-organized, and densely packed³⁶ SAMs formed by thiols on gold electrodes offer advantages such as selectivity, sensitivity, short response time, and small overpotential in electrocatalytic reactions.²⁴ SAM of triazole,²¹ 2-(2,3-dihydroxy phenyl)-1,3-dithiane,²² and L-cysteine¹ modified gold electrodes have been used as biosensors for epinephrine in presence of interfering molecules. Cysteine (Cys), a small thiol-containing amino acid, contains carboxyl, amino and thiol functionalities with respective pK_a values of 1.71, 8.33 and 10.78,³⁷ and is considered perfect in biochemical and electrochemical research.³⁸

Gold nanoparticles have potential applications in the construction of electrochemical sensors and biosensors³⁹ because of their small dimensional size,⁴⁰ good stability, biocompatibility,^{41,42} good conductivity and excellent catalytic activity.^{40,43} On the other hand, gold nanoparticle modifications can greatly increase the immobilized amount of S-functionalized compounds and enhance the Au-S bond and stability of SAMs.² Mercaptopropionic acid, gold nanoparticles and cystamine modified gold electrodes have been applied in voltammetric sensors for simultaneous detection of epinephrine, ascorbic and uric acids.²

Surfactants, a kind of amphiphilic molecules with a hydrophilic head on one side and a long hydrophobic tail on the other, have been widely applied in electrochemistry to improve the property of the electrode/solution interface.^{17,44–50} Also, they have proven effective in the electroanalysis of some biological compounds and drugs.^{46,47} In the presence of sodium dodecylbenzene sulfonate SDBS, the gold nanoparticle modified glassy carbon electrode exhibited good performance in the electrochemical oxidation of tryptophan.⁴⁸ A novel biosensor using poly(3,4-ethylene dioxythiophene) modified Pt electrode was fabricated for selective determination of dopamine,⁴⁴ morphine,⁴⁵ serotonin, and epinephrine¹⁷ in presence of high concentrations of ascorbic and uric acids in the presence of sodium dodecyl sulfate SDS, which forms a monolayer on polymer surface with a high density of negatively charged ends directed outside of the electrode. The electrochemical response of the studied compounds was improved by SDS and the current signal increased due to electrostatic interactions with SDS while the corresponding signals for ascorbic and uric acids were quenched.^{17,44,45}

The aim of the current work is to study the electrochemical behavior of epinephrine at a gold electrode modified with cysteine SAMs over gold nanoparticles. Extensive research has been devoted to self-assembly monolayer adsorption at gold electrodes. However, relatively few publications have addressed SAMs of cysteine on a nanogold particle modified gold electrode and electrochemical behavior and determination of epinephrine in the presence and absence of surfactants at this modified surface.

2. Experimental

2.1. Chemicals and reagents

All chemicals were used without further purification. Epinephrine (EP), ascorbic acid (AA), uric acid (UA), acetaminophen

(APAP), glucose, potassium phosphate (mono, di-basic salt), potassium hydroxide (KOH), cysteine (Cys), sodium dodecyl sulfate (SDS) and hydrogen tetrachloroaurate (HAuCl_4) were supplied by Aldrich Chem. Co. (Milwaukee, WI, USA). Aqueous solutions were prepared using double distilled water. Phosphate buffer solution PBS (1 mol L^{-1} K_2HPO_4 and 1 mol L^{-1} KH_2PO_4) of pH 2–9 was used as the supporting electrolyte. pH was adjusted using 0.1 mol L^{-1} H_3PO_4 and 0.1 mol L^{-1} KOH.

2.2. Electrochemical cells and equipment

Electrochemical deposition and characterization were carried out with a three-electrode/one compartment glass cell. The working electrode was gold (Au) disc (diameter: 1 mm). The auxiliary electrode was in the form of 6.0 cm platinum wire. All the potentials in the electrochemical studies were referenced to Ag/AgCl (4 mol L^{-1} KCl saturated with AgCl) electrode. The working electrode was polished using alumina (2 μM)/water slurry until no visible scratches were observed. Prior to immersion in the cell, the electrode surface was thoroughly rinsed with distilled water and dried. All experiments were performed at $25 \text{ }^\circ\text{C} \pm 0.2 \text{ }^\circ\text{C}$.

The electrosynthesis of the gold nanoparticles and their electrochemical characterization were performed using a BAS-100B electrochemical analyzer (Bioanalytical Systems, BAS, West Lafayette, USA). Quanta FEG 250 instrument was used to obtain the scanning electron micrographs of the different films.

2.3. Electrodeposition of gold nanoparticles

The electrodeposition of gold nanoparticles was achieved in a three-electrode/one compartment electrochemical cell from a solution containing 6 mmol L^{-1} HAuCl_4 and 0.1 mol L^{-1} KNO_3 (prepared in doubly distilled water and deaerated by bubbling with nitrogen). The potential applied between the working electrode (gold electrode) and the reference Ag/AgCl (4 mol L^{-1} KCl saturated with AgCl) electrode is held constant at -400 mV (Bulk electrolysis, BE) for 400 s.³⁹ The surface coverage of gold nanoparticles was $2.042 \times 10^{-6} \text{ mol cm}^{-2}$ (estimated from the quantity of charge used in the electrodeposition process). This electrode is denoted as Au/Au_{nano}.

2.4. Modification of the electrodes by cysteine

A self-assembly monolayer of cysteine was formed on bare Au electrode and gold nanoparticles modified electrode (Au/Au_{nano}) by soaking the electrodes in 5 mmol L^{-1} cysteine/0.1 mol L^{-1} PBS/pH 2.58 for 5 min at room temperature. These electrodes are denoted as Au-Cys, Au/Au_{nano}-Cys, respectively. The modified electrodes were washed with doubly distilled water to remove the physically adsorbed species and dried carefully without touching the surface.

Further modification was carried out by the successive additions of 10 μL of 0.1 mol L^{-1} SDS (prepared in distilled water) to the epinephrine solution (1 mmol L^{-1} EP/0.1 mol L^{-1} PBS/pH 7.40) from 0 up to 130 μL (incremental addition: $6.7 \times 10^{-5} \text{ mol L}^{-1}$ SDS at each addition and the total concentration of SDS after 13 additions is $8.7 \times 10^{-4} \text{ mol L}^{-1}$) and the electrode is denoted as Au/Au_{nano}-Cys...SDS. After each addition, stirring

takes place for 5 min and is then held for 1 min prior to running the experiment.

2.5. Electrochemical impedance spectroscopy

EIS was performed using a Gamry-750 instrument and a lock-in-amplifier that are connected to a personal computer. The data analysis was provided with the instrument and applied non-linear least square fitting with Levenberg–Marquardt algorithm. All impedance experiments were recorded between 0.1 Hz and 100 kHz with an excitation signal of 10 mV amplitude. The measurements were performed under potentiostatic control at different applied potentials which were decided from the cyclic voltammograms recorded for the modified electrodes.

2.6. Analysis of urine

The utilization of the proposed method in real sample analysis was also investigated by direct analysis of EP in human urine samples. EP was dissolved in urine to make a stock solution with 1.3 mmol L^{-1} concentration. Standard additions were carried out from the EP stock solution in 15 mL of 0.1 mol L^{-1} PBS/pH 7.40 containing $130 \mu\text{L}$ 0.1 mol L^{-1} SDS.

3. Results and discussion

3.1. Electrochemical oxidation of epinephrine at the cysteine SAM modified gold electrode

Fig. 1 shows the cyclic voltammetric (CV) behavior of 1 mmol L^{-1} epinephrine (EP) in 0.1 mol L^{-1} PBS/pH 7.40 tested at bare gold electrode Au (solid line) and gold modified with cysteine Au-Cys (dash line). It is clear that the oxidation of EP is irreversible at gold electrodes. At the bare Au electrode, the electrochemical oxidation of EP occurs at approximately 520 mV and the voltammetric peak is rather broad, suggesting slow electron transfer kinetics, presumably due to the fouling of the electrode surface by the oxidation product. However, a relatively well-defined oxidation peak for EP was obtained at the Au-Cys electrode. The oxidation peak potential shifted negatively to 245 mV, and the oxidation peak current increased significantly to $3.9 \mu\text{A}$ at the Au-Cys electrode compared to bare Au electrode. The above results indicate that catalytic effect using the modified electrode facilitates the charge transfer between EP and the modified electrode, and as a result, the electrochemical oxidation of EP becomes easier.

The Au-Cys SAM modified electrode affects the mechanistic redox reaction of EP and there are two types of interactions, the first is the interaction between Au and cysteine through thiol group of cysteine to form strong covalent Au–S bond (substrate-molecule interaction) and the second is between cysteine on Au and EP molecules through the amino group of cysteine and the hydroxyl-phenol group of EP *via* hydrogen bond formation (molecule-molecule interaction) as illustrated in Scheme 1. The electrocatalytic oxidation of EP on Au-Cys is due to the formation of hydrogen bonds between the hydrogen in hydroxyl-phenol of EP and the nitrogen in Cys-SAM. Hydrogen bond formation functions in the activation of hydroxyl-phenol on the benzene ring. As a result, the bond energy between hydrogen and oxygen is weakened and the electron transfer is more liable to

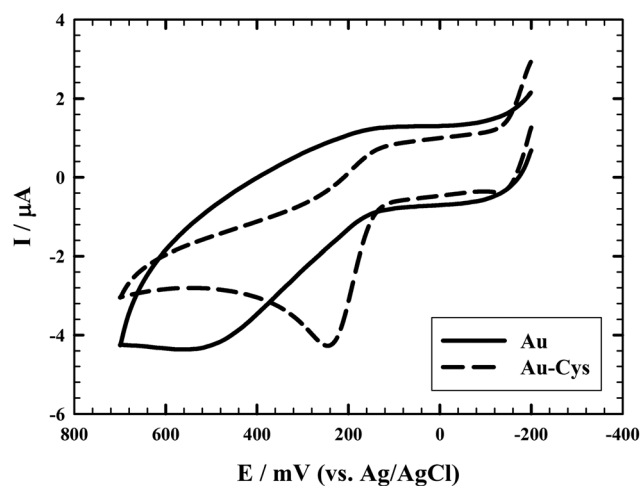


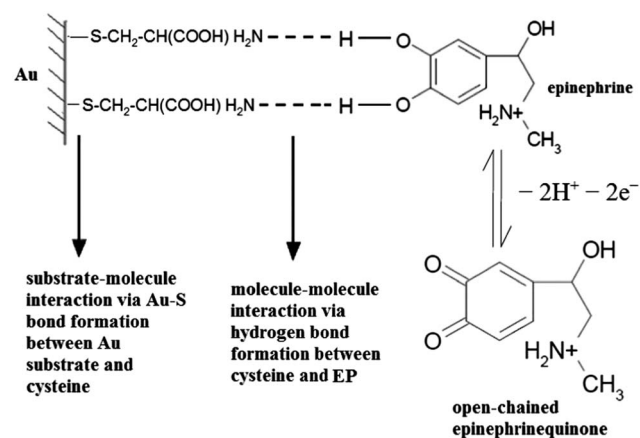
Fig. 1 CVs of 1 mmol L^{-1} EP/ 0.1 mol L^{-1} PBS/pH 7.40 at bare Au (solid line) and Au-Cys (dash line) electrodes, scan rate 50 mV s^{-1} .

occur *via* $\text{N} \cdots \text{H}-\text{O}$ bond. Thus Cys-SAM can act as a promoter to increase the rate of electron transfer and lower the overpotential of EP at the modified electrode.

3.2. Electrochemistry of epinephrine at modified electrodes in presence of SDS

Fig. 2 shows the electrochemistry of EP at different modified electrodes (Au/Au_{nano}, Au/Au_{nano}-Cys, and Au/Au_{nano}-Cys \cdots SDS). Fig. 2(I) shows the electrochemistry of EP at gold nanoparticles modified Au electrode (Au/Au_{nano}), a remarkable increase in the current response ($I_{\text{pa}} = 7.3 \mu\text{A}$) followed by a drop in the oxidation peak potential ($E_{\text{pa}} = 210 \text{ mV}$) are observed due to the catalytic effect of gold nanoparticles which act as a promoter to enhance the electrochemical reaction, considerably accelerating the rate of electron transfer.³⁹

Fig. 2(II) shows the CV of EP at cysteine SAM modified gold nanoparticles (Au/Au_{nano}-Cys). The presence of cysteine SAM on gold nanoparticles leads to a decrease in the oxidation peak current of EP from $7.3 \mu\text{A}$ to $4.7 \mu\text{A}$, and shifts the oxidation



Scheme 1 Schematic model of the electrocatalytic oxidation of EP at Au-Cys electrode *via* substrate-molecule and molecule-molecule interactions.

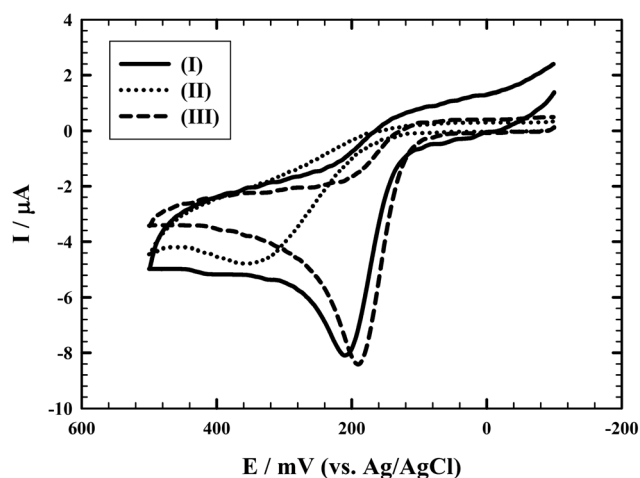
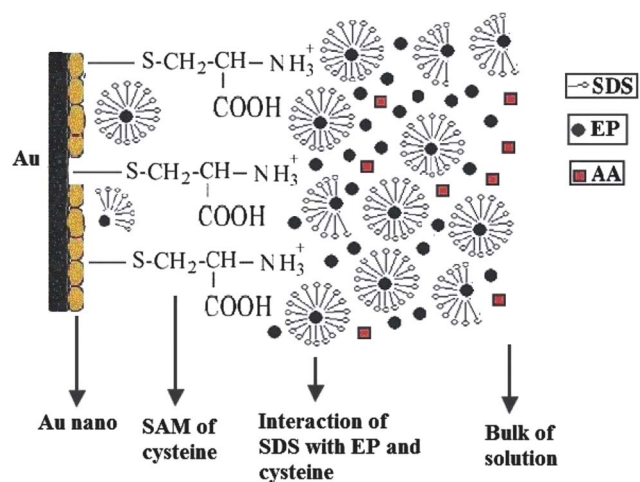


Fig. 2 CVs of 1 mmol L⁻¹ EP/0.1 mol L⁻¹ PBS/pH 7.40 at: (I) Au/Au_{nano}, (II) Au/Au_{nano}-Cys, and (III) Au/Au_{nano}-Cys⋯SDS modified electrodes, scan rate 50 mV s⁻¹.

potential from 210 mV to 358 mV. This is due to; (a) the disorganization of cysteine molecules on gold nanoparticles which inhibits the formation of hydrogen bond between EP and cysteine thus hindering the electron transfer kinetics, (b) electrostatic repulsion between the positively charged cysteine and positively charged EP which hinders EP from reaching the electrode surface.

Fig. 2(III) shows the CV of EP at cysteine SAM modified gold nanoparticles in presence of SDS (Au/Au_{nano}-Cys⋯SDS). Successive additions of 10 μL of 0.1 mol L⁻¹ SDS up to 130 μL (incremental additions: 6.7×10^{-5} mol L⁻¹ SDS at each addition and the total concentration of SDS after 13 additions is 8.7×10^{-4} mol L⁻¹) which leads to increasing oxidation current from 4.7 μA to 8.3 μA, and a shift in the oxidation potential from 358 mV to 190 mV in presence of 130 μL SDS. The schematic model of Au/Au_{nano}-Cys⋯SDS electrode is illustrated in Scheme 2. SDS is an anionic surfactant with hydrophobic tail consisting of 12 carbon atoms and a hydrophilic head that consists of



Scheme 2 Schematic model of Au/Au_{nano}-Cys⋯SDS modified electrode in presence of EP cations and AA.

a sulfate group. There is electrostatic attraction between the cationic EP and the anionic SDS which enhances the diffusion of EP through the positively charged cysteine SAM. Also, there is interaction between the positively charged cysteine and anionic SDS which allows reorganization of cysteine molecules on gold nanoparticles thus enhances hydrogen bond formation between EP and cysteine and promotes faster electron transfer kinetics.

If we compare the CVs of EP at Au-Cys and Au/Au_{nano}-Cys, we conclude that the effect of cysteine on the response of polycrystalline bare Au is more pronounced than that on gold nanoparticles and the effect on gold nanoparticles is enhanced by using SDS which allows reorganization of cysteine on gold nanoparticles to occur and results in the enhancement of the oxidation current and a lowering of the overpotential.

Au/Au_{nano}-Cys in presence of SDS gives beside a higher current response, better stability *via* repeated cycles and long term stability when compared to Au/Au_{nano} thus this work will focus on the Au/Au_{nano}-Cys⋯SDS electrode.

3.3. Stability of the modified electrodes

The stability of the different modified electrodes was studied *via* repeated cycles up to 50 cycles. The inset of Fig. 3 shows the repeated cycle stability of the Au/Au_{nano}-Cys⋯SDS modified electrode. Au/Au_{nano}-Cys, and Au/Au_{nano}-Cys⋯SDS modified electrodes in 1 mmol L⁻¹ EP/0.1 mol L⁻¹ PBS/pH 7.40 give better stability without any noticeable decrease in the current response compared to the Au/Au_{nano} electrode, indicating that these modified electrodes have good reproducibility and do not suffer from surface fouling during repetitive voltammetric measurement due to the formation of a strong Au-S bond.

From CV comparing the 1st, 25th, and 50th cycles of repeated cycles stability of Au/Au_{nano}-Cys electrode (Fig. 3), we observed that I_{pa} increased from 4.9 μA in the 1st cycle up to 8.2 μA in the 25th and 50th cycles, and the oxidation peak potential shifted from 363 mV in the 1st cycle to 220 mV in the 25th and 50th cycles. This indicates that cysteine molecules are reorganized on

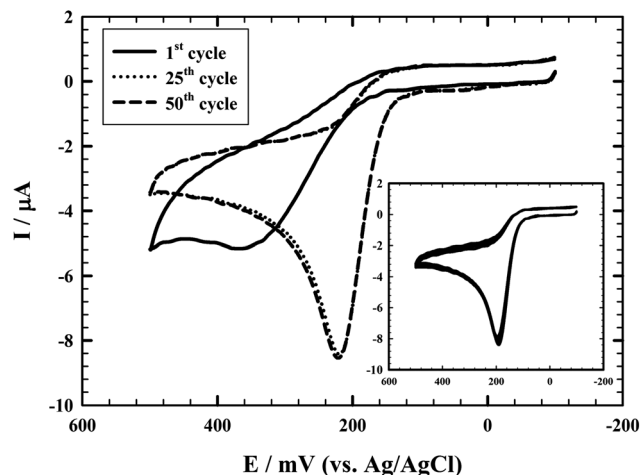


Fig. 3 Comparison of 1st, 25th, and 50th cycles of repeated cycle stability of Au/Au_{nano}-Cys electrode in 1 mmol L⁻¹ EP/0.1 mol L⁻¹ PBS/pH 7.40. Inset: CV of repeated cycles stability of Au/Au_{nano}-Cys⋯SDS modified electrode in 1 mmol L⁻¹ EP, scan rate 50 mV s⁻¹.

gold nanoparticles by repeated cycles and this reorganization enhances the hydrogen bond formation between EP and cysteine which enhances the electron transfer rate. Thus, cysteine molecules are reorganized on gold nanoparticles by repeated cycles or by the addition of SDS (instantaneous reorganization).

Also, the long term stability of Au/Au_{nano}, and Au/Au_{nano}-Cys⋯SDS electrodes was studied for up to one week. After each measurement, the electrode is stored in 0.1 mol L⁻¹ PBS/pH 7.40 in the refrigerator. In case of Au/Au_{nano} electrode, *I*_{pa} of EP decreased by 20%, and 30% after 3 days and one week of storage, respectively. On the other hand, in the case of Au/Au_{nano}-Cys⋯SDS electrode, *I*_{pa} decreased by 9% and 16% after the same periods of storage, respectively. These results indicate that the presence of SAM of cysteine on gold nanoparticles enhances the long term stability of Au/Au_{nano}-Cys⋯SDS electrode due to the formation of strong Au–S bond. Thus, Au/Au_{nano}-Cys⋯SDS electrode current signal is remarkably stable *via* repeated cycles and long term stability, compared to the Au/Au_{nano} electrode.

3.4. Surface morphology of modified electrodes

The response of an electrochemical sensor was related to the physical morphology of its surface. The SEM images of Au/Au_{nano}, Au/Au_{nano}-Cys, and Au/Au_{nano}-Cys⋯SDS electrodes are shown in Fig. 4(A–C), respectively. As observed from SEM images, gold nanoparticles (Fig. 4(A)) are homogeneously distributed and located at different elevations exhibiting a large surface area. On the other hand, gold nanoparticles modified with cysteine SAM (Fig. 4(B)), are randomly distributed on the surface, have dendritic shape and sizes that are not homogenous, but gold nanoparticles modified with cysteine SAM and further modified with SDS (Fig. 4(C)) are homogeneously distributed on the surface, better dispersed and highly packed. The interaction between the anionic SDS and cationic cysteine SAM allows the reorganization and redispersion of gold nanoparticles. Also, a spongy film is observed in Fig. 4(C) due to the surfactant film on the surface which influences the conductivity level of the film and helps the attraction of EP to the electrode surface.

3.5. Effect of scan rate on the voltammetric response of EP

As shown in ESI Fig. 1†, the peak currents (*I*_{pa}) at Au/Au_{nano}-Cys⋯SDS in 1 mmol L⁻¹ EP/0.1 mol L⁻¹ PBS/pH 7.40 varied with change of scan rate. Furthermore, varying the scan rate from 10 to 150 mV s⁻¹ resulted in a positive shift of the oxidation peak potential and an increase of peak current for EP.³⁹ For a diffusion-controlled process,^{2,3,23} a plot of the anodic peak current values *versus* the square root of the scan rate results in a straight-line relationship as shown in the inset of ESI Fig. 1†. The oxidation peak current increased linearly with linear regression eqn (1):

$$I_{pa}(A) = (0.516 \times 10^{-6}) - (3.32 \times 10^{-5}) \nu^{1/2}, (R^2 = 0.9995) \quad (1)$$

at Au/Au_{nano}-Cys⋯SDS, suggesting that the reaction is a diffusion-controlled electrode reaction.

The dependence of the anodic peak current *I*_{pa} (A) on the scan rate has been used for the estimation of the “apparent” diffusion coefficient *D*_{app} of EP. *D*_{app} (cm² s⁻¹) values were calculated from Randles Sevcik equation (2):

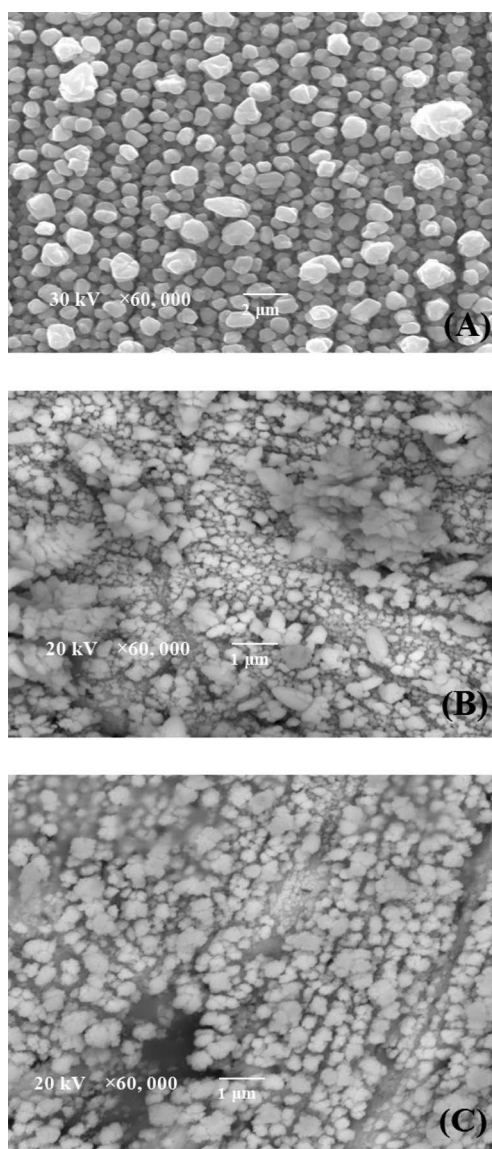


Fig. 4 SEM images of: (A) Au/Au_{nano}, (B) Au/Au_{nano}-Cys, and (C) Au/Au_{nano}-Cys⋯SDS electrodes.

$$I_{pa} = (2.69 \times 10^5) n^{3/2} A C^{\circ} D^{1/2} \nu^{1/2} \quad (2)$$

where *n* is the number of electrons exchanged in oxidation at *T* = 298 K, *A* is the geometrical electrode area = 7.854 × 10⁻³ cm², *C*^o is the analyte concentration (1 × 10⁻⁶ mol cm⁻³) and *ν* is the scan rate V s⁻¹.^{14–16,39} It is important to notice that the apparent surface area used in the calculations does not take into account the surface roughness of the gold nanoparticles (the roughness factor of bare gold and gold nanoparticles calculated from atomic force microscopy measurements are 0.656 and 1.07, respectively).

*D*_{app} value for EP is 1.24 × 10⁻⁵ cm² s⁻¹ at Au/Au_{nano}-Cys, and 3.86 × 10⁻⁵ cm² s⁻¹ at Au/Au_{nano}-Cys⋯SDS. The anionic surfactant SDS affects remarkably the diffusion component of the charge transfer at Au/Au_{nano}-Cys as indicated by the *D*_{app} values. The diffusion coefficient can be considered as an average value of the diffusion process in the bulk, within the surfactant

aggregates in solution and the surfactant layer adsorbed at the surface of the electrode. The values of D_{app} show that the diffusion of EP on Au/Au_{nano}-Cys is enhanced in presence of SDS rather than in absence of it.^{17,44,45}

3.6. Effect of solution pH

Furthermore, pH value of the supporting electrolyte (PBS) is an important parameter in determining the performance of electrochemical sensors.¹⁴ The effect of changing the pH of the supporting electrolyte on the electrochemical response of EP was studied. ESI Fig. 2† shows the CVs of 1 mmol L⁻¹ EP/0.1 mol L⁻¹ PBS of pH 2.58, 4.76, 7.40, and 9.19 at Au/Au_{nano}-Cys⋯SDS modified electrode. It is clear that changing the pH of the supporting electrolyte altered both the peak potential and the peak current of EP indicating that the electrocatalytic oxidation of EP at the Au/Au_{nano}-Cys⋯SDS is a pH-dependent reaction and protonation/deprotonation takes part in the charge transfer process. The anodic peak potential shifted negatively with the increase in the solution pH.^{14,39}

Fig. 5 shows the linear relationship between the solution pH value and the anodic peak potential of EP at Au/Au_{nano}-Cys electrode in absence (a) and in presence (b) of SDS over the pH range 2.58 to 9.19. In general, the oxidation peak potential shifts to more positive values as the pH decreases in the absence and presence of SDS.⁴⁴ A slope of -0.069 V/pH units, which is close to the theoretical value of -0.059 V/pH was obtained at Au/Au_{nano}-Cys⋯SDS, indicating that the overall process is proton dependent with an equal number of protons and electrons involved in EP oxidation.^{2,3,7} As EP oxidation is a two-electron process, the number of protons involved is also predicted to be two indicating a $2e^-/2H^+$ process.^{8,21,23}

The inset of Fig. 5 shows the relationship between the solution pH value and the anodic peak current of EP at Au/Au_{nano}-Cys electrode in absence (a) and in presence (b) of SDS. The anodic peak current increased from pH 2.58 to pH 7.40 where it reached its maximum value and decreased again at pH 9.19. In solution,

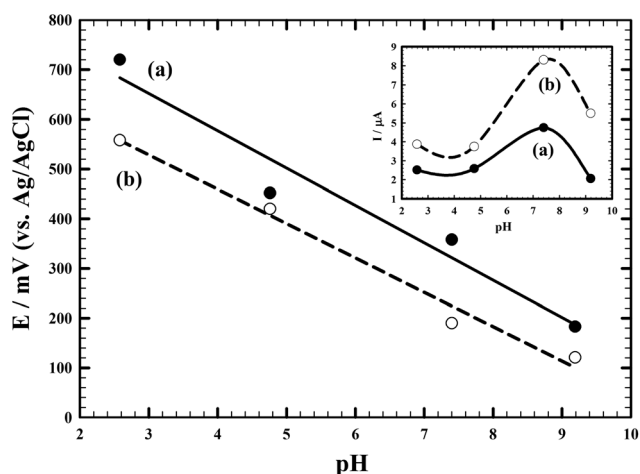


Fig. 5 Dependence of the anodic peak potential of 1 mmol L⁻¹ EP/0.1 mol L⁻¹ PBS on pH value of the solution at Au/Au_{nano}-Cys in absence (a) and presence (b) of SDS. Inset; dependence of the anodic peak current of EP on pH value of the solution at Au/Au_{nano}-Cys electrode in absence (a) and presence (b) of SDS.

the pK_a value of EP is 8.55. The deprotonation of EP occurs at pH 9.19, and it is no longer a two-proton, two-electron process at this point and other equilibria should be taken into account, thus the anodic peak current decreased at pH 9.19. The highest oxidation peak current was obtained at pH 7.40 (pH medium of the human body). Thus PBS/pH 7.40 was employed for the determination of EP to achieve higher sensitivity.^{5,6}

3.7. Determination of EP at physiological pH using Au/Au_{nano}-Cys in presence of SDS

The voltammetric behavior of EP was examined using linear sweep voltammetry (LSV) with a scan rate 50 mV s⁻¹. Inset (2) in Fig. 6 shows typical LSV of standard additions of 0.5 mmol L⁻¹ EP/0.1 mol L⁻¹ PBS/pH 7.40 to 130 μL of 0.1 mol L⁻¹ SDS in 15 mL of 0.1 mol L⁻¹ PBS/pH 7.40, indicating that by increasing the concentration of EP, the anodic peak current increases which indicates that the electrochemical response of EP is apparently improved by SDS due to the enhanced accumulation of protonated EP *via* electrostatic interaction with negatively charged SDS at the Au/Au_{nano}-Cys electrode surface.

Fig. 6 inset (1) shows the calibration curves of the anodic peak current values of EP in the linear range of 35 μmol L⁻¹ to 200 μmol L⁻¹ with the regression equation of I_p (A) = $1.005 \times 10^{-8} c(\mu\text{mol L}^{-1}) + (7.016 \times 10^{-9})$ and from 2 μmol L⁻¹ to 30 μmol L⁻¹ EP with the regression equation I_p (A) = $1.019 \times 10^{-8} c(\mu\text{mol L}^{-1}) + (1.410 \times 10^{-8})$. The correlation coefficients of 0.9999, and 0.9981, sensitivities of 0.01005 μA μmol⁻¹ L⁻¹, and 0.01019 μA μmol⁻¹ L⁻¹, detection limits of 1.49 nmol L⁻¹ and 0.294 nmol L⁻¹, and quantification limits of 4.97 nmol L⁻¹ and 0.981 nmol L⁻¹, respectively have been obtained. The detection limit (DL) and quantification limit (QL) were calculated from the equations: DL = $3s/b$, and QL = $10s/b$, respectively, where s is the standard deviation and b is the slope of the calibration curve. Table 1 shows the comparison for the determination of EP at Au/Au_{nano}-Cys⋯SDS electrode with various modified electrodes based on literature reports.

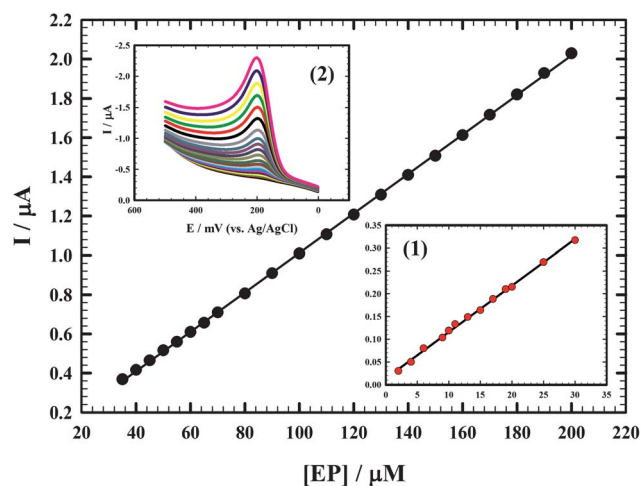


Fig. 6 Calibration curve for EP for concentrations from (35 μmol L⁻¹ to 200 μmol L⁻¹) and from (2 μmol L⁻¹–30 μmol L⁻¹, inset 1), inset (2); LSVs of 15 ml of 0.1 mol L⁻¹ PBS/pH 7.40 at Au/Au_{nano}-Cys⋯SDS in different concentrations of EP (2 μmol L⁻¹–200 μmol L⁻¹), scan rate 50 mV s⁻¹.

Table 1 Comparison for determination of EP at various modified electrodes based on literature reports^a

Electrode	pH	LDR (μM)	Sensitivity ($\mu\text{A } \mu\text{M}^{-1}$)	LOD (nM)	Reference
PPy/AuNPs/SWCNTs-AuE	7.0	0.004–0.1	NR	2	5
L-Cys/Au SAMs	7.0	0.1–2	0.7125	10	1
Au/Au-NPs/MPA/CA/Au-NPs	7.0	0.1–800	1.5	40	2
TA SAM/Au	4.4	0.1–10	0.083	10	21
Nano-Au/CA/GC	7.0	0.1–500	0.376	40	23
DPD-Au	8.0	0.7–500	0.01	510	22
Au/Au _{nano} -Cys...SDS	7.4	2–30	0.0102	0.294	This work

^a Note. LDR, linear dynamic range; LOD, limit of detection; NR, not reported; PPy, polypyrrole; AuNPs, gold nanoparticles; SWCNTs, single-walled carbon nanotubes; AuE, gold electrode; L-Cys, L-cysteine; SAMs, self-assembly monolayers; MPA, Mercaptopropionic acid; CA, cystamine; TA, 3-amino-5-mercapto-1,2,4-triazole; GC, glassy carbon; DPD, 2-(2,3-dihydroxy phenyl)-1,3-dithiane.

3.8. Determination of EP in human urine samples

The determination of EP in urine samples is of medical importance so the utilization of the proposed method in real sample analysis was investigated by direct analysis of EP in human urine. The same measurements were conducted successfully on urine samples. In this set of experiments, EP was dissolved in urine to make a stock solution with 0.5 mmol L^{-1} concentration and typical LSVs of standard additions of 0.5 mmol L^{-1} EP in urine to $130 \mu\text{L}$ of 0.1 mol L^{-1} SDS in 15 mL of 0.1 mol L^{-1} PBS/pH 7.40 at Au/Au_{nano}-Cys were obtained (figure not shown). The calibration curves of EP in urine in the linear range of $25 \mu\text{mol L}^{-1}$ to $200 \mu\text{mol L}^{-1}$, and $3 \mu\text{mol L}^{-1}$ – $20 \mu\text{mol L}^{-1}$ are shown in ESI Fig. 3 and inset†, respectively. The detection limits of 1.93 nmol L^{-1} , and $0.472 \text{ nmol L}^{-1}$ with correlation coefficients of 0.999, and 0.996 were obtained, respectively.

Five different concentrations on the calibration curve were chosen to be repeated to evaluate the accuracy and precision of the proposed method, which is represented in Table 2. The recovery ranged from 98.2% to 100.1%, and the results are acceptable indicating that the present procedures are free from interferences of the urine sample matrix. The results strongly proved that EP can be selectively and sensitively determined at Au/Au_{nano}-Cys...SDS modified electrode in urine sample.

3.9. Interference study

In the electrochemical determinations of EP in clinical preparations, presence of some potentially interfering compounds is considered as a significant problem in accuracy of determination. These compounds generally show overlapping signals on the surface of most chemically modified electrodes, which limit the analytical applicability of the sensors.⁸ The inset of Fig. 7(A) shows the LSVs of 1 mmol L^{-1} EP and 1 mmol L^{-1} APAP in 0.1 mol L^{-1} PBS/pH 7.40 at Au/Au_{nano}-Cys in absence (solid line)

and presence (dash line) of SDS. In absence of SDS, two resolved peaks at 222 mV and 431 mV were obtained for EP and APAP, respectively. But, in presence of SDS, there is an observable increase in the oxidation peak current of EP from $4.42 \mu\text{A}$ in absence of SDS to $8.14 \mu\text{A}$ in presence of SDS due to the electrostatic interaction of the anionic surfactant with the protonated EP ($\text{p}K_{\text{a}} = 8.55$), and a decrease in the oxidation current of APAP. The decrease in the anodic peak current of APAP may be attributed firstly to its structure in which it behaves neutral in the pH of study ($\text{p}K_{\text{a}} = 9.5$), and its diffusion towards the Au/Au_{nano}-Cys electrode is slow in comparison with other cationic compounds. Secondly, its interaction with the anionic SDS is retarded as it becomes a neutral compound. Thus, Au/Au_{nano}-Cys...SDS modified electrode can be used for the simultaneous determination of binary mixture of EP and APAP.

On the other hand, it is well known that UA coexists with EP in the extracellular fluid of the central nervous system and its concentration is higher than that of EP. Since, UA is an important interfering substance for the electrochemical analysis of EP, the interference from UA was investigated. Fig. 7(A) shows the LSVs of 0.5 mmol L^{-1} EP and 1 mmol L^{-1} UA in presence of 5 mmol L^{-1} glucose in 0.1 mol L^{-1} PBS/pH 7.40 at Au/Au_{nano}-Cys modified electrode in absence (a) and presence of SDS (b). It is clear that no interference could be observed from glucose at the modified electrode in absence or in presence of SDS. At Au/Au_{nano}-Cys modified electrode, two well separated oxidation peaks were obtained at 212 mV and 418 mV for EP and UA, respectively. By successive additions of SDS, the oxidation peak current for EP increased from $4.07 \mu\text{A}$ in absence of SDS to $6.01 \mu\text{A}$ in presence of SDS, while the oxidation peak current for UA decreased. The high response for EP was observed due to the electrostatic interaction of the anionic surfactant with the protonated EP ($\text{p}K_{\text{a}} = 8.55$) in pH 7.40, but in case of UA repulsion takes place as UA ($\text{p}K_{\text{a}} = 5.4$) is in the anionic form and in micellar medium they established an electrostatic

Table 2 Evaluation of the accuracy and precision of the proposed method for the determination of EP in urine sample

Sample	Concentration of EP added ($\mu\text{mol L}^{-1}$)	Concentration of found EP ($\mu\text{mol L}^{-1}$)	Recovery (%)	Standard deviation $\times 10^{-8}$	Standard error $\times 10^{-8}$
1	11.0	10.8	98.2	0.136	0.0609
2	30.0	29.6	98.7	0.339	0.152
3	100	99.9	99.9	0.231	0.103
4	140	140.1	100.1	0.710	0.318
5	200	199.7	99.9	0.283	0.126

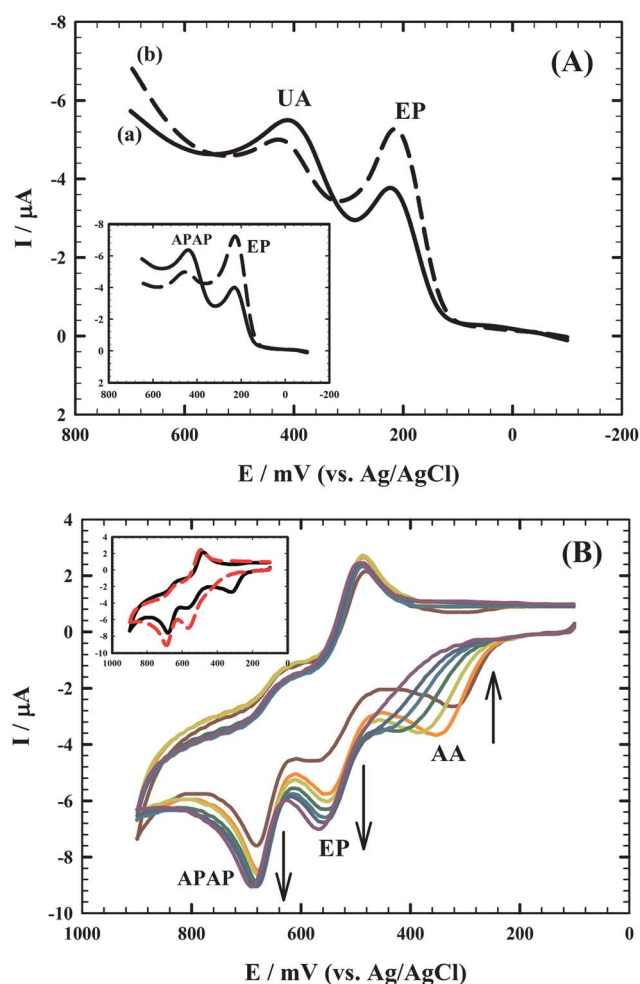


Fig. 7 (A) LSV of 0.5 mmol L⁻¹ EP, 1 mmol L⁻¹ UA in presence of 5 mmol L⁻¹ glucose in 0.1 mol L⁻¹ PBS/pH 7.40 at (a) Au/Au_{nano}-Cys and (b) Au/Au_{nano}-Cys⋯SDS; inset; LSV of 1 mmol L⁻¹ EP, 1 mmol L⁻¹ APAP/0.1 mol L⁻¹ PBS/pH 7.40 at Au/Au_{nano}-Cys (solid line) and Au/Au_{nano}-Cys⋯SDS (dash line), (B) CVs of 1 mmol L⁻¹ AA, 1 mmol L⁻¹ EP and 1 mmol L⁻¹ APAP in 0.1 mol L⁻¹ PBS/pH 2.58 at Au/Au_{nano}-Cys with successive additions of (0–130 μL) 0.1 mol L⁻¹ SDS, the inset represents the initial (in absence of SDS) and final (in presence of 130 μL SDS) CVs, scan rate 50 mV s⁻¹.

repulsion with anionic surfactant SDS, which provokes a decrease in the peak current value. This indicates that the accumulation of SDS on the modified electrode forms a negative layer on the electrode surface. Therefore, we can determine EP selectively in the presence of UA and glucose. The change of the peak current values for UA and EP after adding SDS can be assigned to the spontaneous adsorption of the surfactant onto electrode surface, which may change the overpotential of the electrode and influence the electron transfer rate. Also, the formation of micellar aggregates may influence the mass transport of electroactive species to the electrode.⁴⁴

3.10. Analysis of tertiary mixture at Au/Au_{nano}-Cys modified electrode in presence of SDS

EP and AA always exist together in biological environment. Simultaneous determination of EP and AA is difficult at bare

gold electrode due to the overlapping of their signals. But the peak potentials can be distinguished at Au/Au_{nano}-Cys modified electrode. According to the remarkable effect of pH on the oxidation peak potential, there was a good separation of peak potentials in PBS/pH 2.58, so we chose pH 2.58 in the simultaneous determination of EP and AA.²¹ Moreover, acetaminophen (paracetamol), APAP, is likely to interfere with AA determination.^{15,16} Fig. 7(B) shows the CVs of tertiary mixture of 1 mmol L⁻¹ AA, 1 mmol L⁻¹ EP and 1 mmol L⁻¹ APAP in 0.1 mol L⁻¹ PBS/pH 2.58 at Au/Au_{nano}-Cys with successive additions of (0–130) μL of 0.1 mol L⁻¹ SDS. The inset of Fig. 7(B) shows the CVs of the mixture (AA, EP, and APAP) in the absence and presence of SDS. Three well-defined oxidation peaks were obtained at Au/Au_{nano}-Cys modified electrode at 321, 580, and 680 mV for AA, EP, and APAP, respectively. The large separation of the peak potentials allows selective and simultaneous determination of AA, EP, and APAP in their mixtures at the Au/Au_{nano}-Cys electrode. By successive additions of 10 μL of 0.1 mol L⁻¹ SDS in the mixture solution, the oxidation peak current of EP and APAP increases while the oxidation peak current of AA decreases until it completely disappears.

Surfactants tend to adsorb at different interfaces at concentrations below and/or above the critical micellar concentration. Thus, it is expected that the addition of SDS will result in the formation of a surfactant film over the Au/Au_{nano}-Cys electrode. This amphiphilic film will align in a way where the head groups of surfactant molecules face the aqueous medium leaving the rest hydrophobic part in contact with each other and away from the aqueous medium. It is clear that there is a negatively charged surface; behind this negative surface there is a hydrophobic region due to the alignment of the surfactant tails. Consequently, the negative charge of the adsorbed surfactant film as well as the hydrophobic character of the interior of the film will act to repel hydrophilic AA molecules or the AA⁻ away from the electrode surface while enhancing the preconcentration/accumulation of the hydrophobic cations of EP and APAP as illustrated in

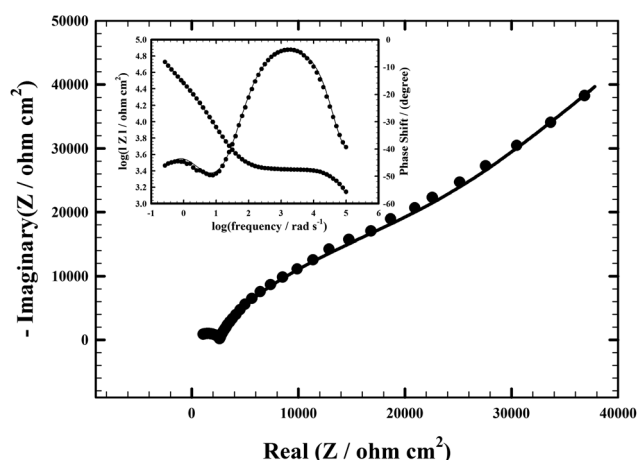


Fig. 8 Nyquist plot of Au/Au_{nano}-Cys⋯SDS modified electrode in 1 mmol L⁻¹ EP/0.1 mol L⁻¹ PBS/pH 7.40 at the oxidation potential (200 mV) and inset, the typical impedance spectrum presented in the form of Bode plot. (Symbols and solid lines represent the experimental measurements and the computer fitting of impedance spectra, respectively), frequency range: 0.1–100 000 Hz.

Table 3 EIS fitting data corresponding to Fig. 8

$R_{L1}/$ ($10^3 \Omega \text{ cm}^2$)	$R_{L2}/$ ($10^3 \Omega \text{ cm}^2$)	$R_{ct}/$ ($10^4 \Omega \text{ cm}^2$)	$C_{c3}/$ ($10^{-6} \text{ F cm}^{-2}$)	$R_s/$ ($10^2 \Omega \text{ cm}^2$)	$C_{c2}/$ ($10^{-9} \text{ F cm}^{-2}$)	CPE1/ (10^5 F cm^{-2})	$n1$	Z ($10^5 \Omega \text{ s}^{-1/2}$)
8.337	2.591	4.343	2.740	5.609	1.491	1.750	0.8036	1.047

Scheme 2.⁴⁴ Thus Au/Au_{nano}-Cys⋯SDS modified electrode can be used for the selective determination of AA, EP, and APAP in the mixtures.

3.11. Electrochemical impedance spectroscopy (EIS) of EP

EIS is regarded as an effective method to monitor the interfacial properties of surface-modified electrodes.^{39,44,45} Therefore, EIS was used to investigate the nature of EP interaction at Au/Au_{nano}-Cys⋯SDS surface. EIS data are obtained for the modified electrode at ac frequency varying between 0.1 Hz and 100 kHz with an applied potential (200 mV) in the region corresponding to the electrolytic oxidation of EP in 0.1 mol L⁻¹ PBS/pH 7.40. Fig. 8 shows a typical impedance spectrum presented in the form of Nyquist plot of EP at Au/Au_{nano}-Cys⋯SDS electrode and the inset shows the typical impedance spectrum presented in the form of Bode plot. The experimental data were compared to an equivalent circuit that used some of the conventional circuit elements, namely; resistance, capacitance, diffusion, and induction elements.^{14,39} The equivalent circuit is shown in ESI Fig. 4†. In this circuit, R_s is the solution resistance, R_{L1} is the resistance due to the surfactant film on the surface, R_{L2} is the resistance due to the SAM of cysteine, and R_{ct} is the charge transfer resistance. Capacitors in EIS experiments do not behave ideally; instead they act like a constant phase element (CPE). Therefore, CPE1 is a constant phase element and $n1$ is its corresponding exponent (n is less than one). C_{c2} and C_{c3} represent the capacitance of the double layer. Diffusion can create an impedance known as the Warburg impedance Z . Table 3 lists the best fitting values calculated from the equivalent circuit for the impedance data of Fig. 8.

As shown in Fig. 8, the impedance spectra include a semicircle portion and a linear portion; the semicircle part at the higher frequencies corresponding to the electron-transfer limiting electrochemical process, and the linear part at the lower frequencies corresponding to the diffusion-limiting electrochemical process. The semicircle diameter equals the interfacial charge transfer resistance R_{ct} . This resistance controls the electron transfer kinetics of the redox probe at the electrode interface. Therefore, R_{ct} can be used to describe the interface properties of the electrode.¹⁸ The semicircle part in Fig. 8 diminishes markedly, implying a low charge transfer resistance R_{ct} of the redox probe. This is attributed to the selective interaction between SDS and EP that resulted in the observed current signal increase for the electro-oxidation process. This indicates the conductivity and the high catalytic activity of the modified electrode and the facilitation of charge transfer. The values of the capacitive component indicating the conducting character of the modified surface due to ionic adsorption at the electrode surface and the charge transfer process.

3.12. Oxidative and reductive desorption of cysteine SAM

The electrochemical desorption experiment can be used to confirm the formation of SAM of alkanethiols on gold nanoparticles modified electrode and bare gold electrode *via* the S–Au bond. Porter and coworkers suggested that alkanethiol monolayers on gold electrodes were both oxidatively and reductively desorbed.^{24,28,51} Fig. 9 shows the oxidative desorption of Au-Cys (a) and Au/Au_{nano}-Cys (b) electrodes in 0.1 mol L⁻¹ PBS/pH 2.58. The oxidative desorption of SAMs from bare gold and gold nanoparticles modified electrode elucidates that gold nanoparticles could not only increase the assembly amount of cysteine but also influence the structure and stability of SAM.⁵¹

Thiols are reductively desorbed by the following reaction²⁸ in alkaline solutions through a one-electron reduction reaction eqn (3):^{24,26,51}



The surface concentration of the thiulates can be roughly determined from the charge consumed during the reductive desorption.²⁶ The inset of Fig. 9 shows the reductive desorption of Au-Cys (solid line) and Au/Au_{nano}-Cys (dash line) in 0.5 mol L⁻¹ KOH. Two cathodic peaks are obtained at -736 mV and -1027 mV at bare gold and at -720 mV and -1008 mV at gold nanoparticles modified electrode. The desorption peak current increased largely as a result of gold nanoparticles deposition.⁵¹ Wenrong Yang *et al.* proposed that the first peak (Q1) is due to the cleavage of the Au–S bond (having a shape characteristic of an adsorbed species), and the second peak (Q2), having more

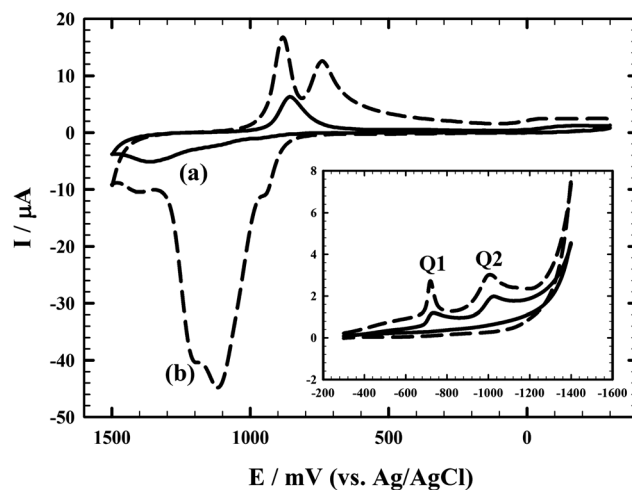


Fig. 9 CVs of the oxidative desorption of Au-Cys (a) and Au/Au_{nano}-Cys (b) in 0.1 mol L⁻¹ PBS/pH 2.58, inset; CVs of the reductive desorption of Au-Cys (solid line) and Au/Au_{nano}-Cys (dash line) in 0.5 mol L⁻¹ KOH, scan rate 50 mV s⁻¹.

diffusion-like character is possibly due to a similar field-induced rearrangement of cysteine clusters which would occur within the electrical double layer. The surface coverage of cysteine was therefore determined from the area under the first peak (Q1).²⁸ By integrating the current under the first cathodic wave (Q1), the estimated surface coverage for the cysteine SAM is 2.64×10^{-9} mol cm⁻² on bare gold and 4.43×10^{-9} mol cm⁻² on gold nanoparticles modified electrode. Thus gold nanoparticle modification can greatly increase the immobilization amount of cysteine and enhance the Au-S bond and stability of cysteine SAM.⁵¹

4. Conclusion

In the present work, the difference in the electrochemical behavior of SAMs of cysteine at bare Au and Au/Au_{nano} is compared for the first time. Oxidative and reductive desorption proved conclusively that cysteine has self-assembled on the bare Au and Au/Au_{nano} surfaces to form monolayers through Au-S strong interactions. Gold nanoparticles modification can greatly increase the immobilization amount of cysteine and enhance the Au-S bond and stability of cysteine SAM. Au/Au_{nano}-Cys \cdots SDS can selectively determine epinephrine in presence of a large amount of UA and glucose. Also, we demonstrated the selective and simultaneous determination of tertiary mixture of AA, EP, and APAP using Au/Au_{nano}-Cys \cdots SDS. A novel approach for the utilization of anionic surfactants in electroanalytical applications is described in this work. The negatively charged SDS adsorbed onto the electrode surface controls the electrode reactions of AA, EP, and APAP that differ in their net charge. The negative charge of the adsorbed surfactant film as well as the hydrophobic character of the interior of the film will act to repel hydrophilic AA molecules or their corresponding AA⁻ away from the electrode surface while enhancing the preconcentration/accumulation of hydrophobic cations of EP and APAP. Au/Au_{nano}-Cys \cdots SDS gives better stability *via* repeated cycles and long term stability due to the formation of strong Au-S bond. The proposed method was simple, sensitive, and successfully applied for determination of EP in human urine with good precision and accuracy. The present modified electrode showed high reproducibility, sensitivity, selectivity, and better stability.

Acknowledgements

The authors would like to acknowledge the financial support from Cairo University through the Vice President Office for Research Funds.

References

- 1 S.-f. Wang, D. Du and Q.-C. Zou, Electrochemical behavior of epinephrine at L-cysteine self-assembled monolayers modified gold electrode, *Talanta*, 2002, **57**, 687–692.
- 2 T. Luczak, Comparison of electrochemical oxidation of epinephrine in the presence of interfering ascorbic and uric acids on gold electrodes modified with S-functionalized compounds and gold nanoparticles, *Electrochim. Acta*, 2009, **54**, 5863–5870.
- 3 S. Shahrokhiana, M. Ghalkhania and M. K. Amini, Application of carbon-paste electrode modified with iron phthalocyanine for voltammetric determination of epinephrine in the presence of ascorbic acid and uric acid, *Sens. Actuators, B*, 2009, **137**, 669–675.
- 4 H. E. Bouhouti, I. Naranjo Rodriguez, J. L. H. d. Cisneros, M. ElKaoutit, K. R. Temsamani, D. Bouchta and L. M. C. Aguilera, Electrochemical behaviour of epinephrine and uric acid at a sonogel-carbon L-cysteine modified electrode, *Talanta*, 2009, **79**, 22–26.
- 5 X. Lu, Y. Li, J. Du, X. Zhou, Z. Xue, X. Liu and Z. Wang, A novel nanocomposites sensor for epinephrine detection in the presence of uric acids and ascorbic acids, *Electrochim. Acta*, 2011, **56**, 7261–7266.
- 6 Y. Zeng, J. Yang and K. Wu, Electrochemistry and determination of epinephrine using a mesoporous Al-incorporated SiO₂ modified electrode, *Electrochim. Acta*, 2008, **53**, 4615–4620.
- 7 S. Shahrokhian and M. Khafaji, Application of pyrolytic graphite modified with nano-diamond/graphite film for simultaneous voltammetric determination of epinephrine and uric acid in the presence of ascorbic acid, *Electrochim. Acta*, 2010, **55**, 9090–9096.
- 8 S. Shahrokhian and R.-S. Saberi, Electrochemical preparation of over-oxidized polypyrrole/multi-walled carbon nanotube composite on glassy carbon electrode and its application in epinephrine determination, *Electrochim. Acta*, 2011, **57**, 132–138.
- 9 M. Zhou, L.-P. Guo, Y. Hou and X.-J. Peng, Immobilization of Nafion-ordered mesoporous carbon on a glassy carbon electrode: application to the detection of epinephrine, *Electrochim. Acta*, 2008, **53**, 4176–4184.
- 10 Y. Wang and Z.-z. Chen, A novel poly(taurine) modified glassy carbon electrode for the simultaneous determination of epinephrine and dopamine, *Colloids Surf., B*, 2009, **74**, 322–327.
- 11 J. Bai, B. Lu, X. Bo and L. Guo, Electrochemical property and electroanalytical application of large mesoporous carbons, *Electrochem. Commun.*, 2010, **12**, 1563–1567.
- 12 F. Arduini, A. Amine, C. Majorani, F. D. Giorgio, D. D. Felicis, F. Cataldo, D. Moscone and G. Palleschi, High performance electrochemical sensor based on modified screen-printed electrodes with cost-effective dispersion of nanostructured carbon black, *Electrochem. Commun.*, 2010, **12**, 346–350.
- 13 Y. Li, Y. Umasankar and S.-M. Chen, Multiwalled carbon nanotubes with poly(NDGACHi) biocomposite film for the electrocatalysis of epinephrine and norepinephrine, *Anal. Biochem.*, 2009, **388**, 288–295.
- 14 N. F. Atta, M. F. El-Kady and A. Galal, Simultaneous determination of catecholamines, uric acid and ascorbic acid at physiological levels using poly(N-methylpyrrole)/Pd-nanoclusters sensor, *Anal. Biochem.*, 2010, **400**, 78–88.
- 15 N. F. Atta, M. F. El-Kady and A. Galal, Palladium nanoclusters-coated polyfuran as a novel sensor for catecholamine neurotransmitters and paracetamol, *Sens. Actuators, B*, 2009, **141**, 566–574.
- 16 N. F. Atta and M. F. El-Kady, Poly(3-methylthiophene)/palladium sub-micro-modified sensor electrode. Part II: voltammetric and EIS studies, and analysis of catecholamine neurotransmitters, ascorbic acid and acetaminophen, *Talanta*, 2009, **79**, 639–647.
- 17 N. F. Atta, A. Galal and R. A. Ahmed, Simultaneous determination of catecholamines and serotonin on poly(3,4-ethylenedioxythiophene) modified Pt electrode in presence of sodium dodecyl sulfate, *J. Electrochem. Soc.*, 2011, **158**(4), F52–F60.
- 18 N. F. Atta, A. Galal, F. M. Abu-Attia and S. M. Azab, Simultaneous determination of paracetamol and neurotransmitters in biological fluids using a carbon paste sensor modified with gold nanoparticles, *J. Mater. Chem.*, 2011, **21**, 13015–13024.
- 19 J. Li and X.-Q. Lin, Electrodeposition of gold nanoclusters on overoxidized polypyrrole film modified glassy carbon electrode and its application for the simultaneous determination of epinephrine and uric acid under coexistence of ascorbic acid, *Anal. Chim. Acta*, 2007, **596**, 222–230.
- 20 F. C. Moraes, D. L. C. Golinelli, L. H. Mascaro and S. A. S. Machado, Determination of epinephrine in urine using multi-walled carbon nanotube modified with cobalt phthalocyanine in a paraffin composite electrode, *Sens. Actuators, B*, 2010, **148**, 492–497.
- 21 Y.-X. Sun, S.-F. Wang, X.-H. Zhang and Y.-F. Huang, Simultaneous determination of epinephrine and ascorbic acid at the electrochemical sensor of triazole SAM modified gold electrode, *Sens. Actuators, B*, 2006, **113**, 156–161.
- 22 M. Mazloum Ardakani, H. Beitollahi, M. K. Amini, B.-F. Mirjalili and F. Mirkhalaf, Simultaneous determination of epinephrine and uric acid at a gold electrode modified by a 2-(2,3-dihydroxy

- phenyl)-1,3-dithiane self-assembled monolayer, *J. Electroanal. Chem.*, 2011, **651**, 243–249.
- 23 Z. Yang, G. Hu, X. Chen, J. Zhao and G. Zhao, The nano-Au self-assembled glassy carbon electrode for selective determination of epinephrine in the presence of ascorbic acid, *Colloids Surf., B*, 2007, **54**, 230–235.
 - 24 R. K. Shervedani, M. Bagherzadeh and S. A. Mozaffari, Determination of dopamine in the presence of high concentration of ascorbic acid by using gold cysteamine self-assembled monolayers as a nanosensor, *Sens. Actuators, B*, 2006, **115**, 614–621.
 - 25 X.-H. Zhang and S.-F. Wang, Determination of ethamsylate in the presence of catecholamines using 4-amino-2-mercaptopyrimidine self-assembled monolayer gold electrode, *Sens. Actuators, B*, 2005, **104**, 29–34.
 - 26 Y. Chen, L.-R. Guo, W. Chen, X.-J. Yang, B. Jin, L.-M. Zheng and X.-H. Xia, 3-mercaptopropylphosphonic acid modified gold electrode for electrochemical detection of dopamine, *Bioelectrochemistry*, 2009, **75**, 26–31.
 - 27 M. J. Giz, B. Duong and N. J. Tao, In situ STM study of self-assembled mercaptopropionic acid monolayers for electrochemical detection of dopamine, *J. Electroanal. Chem.*, 1999, **465**, 72–79.
 - 28 W. Yang, J. J. Gooding and D. B. Hibbert, Characterisation of gold electrodes modified with self-assembled monolayers of L-cysteine for the adsorptive stripping analysis of copper, *J. Electroanal. Chem.*, 2001, **516**, 10–16.
 - 29 G. Dodero, L. D. Michieli, O. Cavalleri, R. Rolandi, L. Oliveri, A. Daccà and R. Parodi, L-Cysteine chemisorption on gold: an XPS and STM study, *Colloids Surf., A*, 2000, **175**, 121–128.
 - 30 M. S. El-Deab and T. Ohsaka, Quasi-reversible two-electron reduction of oxygen at gold electrodes modified with a self-assembled submonolayer of cysteine, *Electrochem. Commun.*, 2003, **5**, 214–219.
 - 31 Y. Zhao, J. Bai, L. Wang, X. E. P. Huang, H. Wang and L. Zhang, Simultaneous electrochemical determination of uric acid and ascorbic acid using L-cysteine self-assembled gold electrode, *Int. J. Electrochem. Sci.*, 2006, **1**, 363–371.
 - 32 A.-S. Duwez, Exploiting electron spectroscopies to probe the structure and organization of self-assembled monolayers: a review, *J. Electron Spectrosc. Relat. Phenom.*, 2004, **134**, 97–138.
 - 33 Q. Wang, N. Jiang and N. Li, Electrocatalytic response of dopamine at a thiolactic acid self-assembled gold electrode, *Microchem. J.*, 2001, **68**, 77–85.
 - 34 E. Briand, M. Salmain, C. Compère and C.-M. Pradier, Immobilization of Protein A on SAMs for the elaboration of immunosensors, *Colloids Surf., B*, 2006, **53**, 215–224.
 - 35 S. Wang and D. Du, Studies on the electrochemical behaviour of hydroquinone at L-cysteine self-assembled monolayers modified gold electrode, *Sensors*, 2002, **2**, 41–49.
 - 36 Y. Saga and H. Tamiaki, Facile synthesis of chlorophyll analog possessing a disulfide bond and formation of self-assembled monolayer on gold surface, *J. Photochem. Photobiol., B*, 2004, **73**, 29–34.
 - 37 G. Hager and A. G. Brolo, Adsorption/desorption behaviour of cysteine and cystine in neutral and basic media: electrochemical evidence for differing thiol and disulfide adsorption to a Au(1 1 1) single crystal electrode, *J. Electroanal. Chem.*, 2003, **550–551**, 291–301.
 - 38 S. Aryal, B. K. C. Remant, N. Dharmaraj, N. Bhattarai, C. H. Kim and H. Y. Kim, Spectroscopic identification of S Au interaction in cysteine capped gold nanoparticles, *Spectrochim. Acta, Part A*, 2006, **63**, 160–163.
 - 39 N. F. Atta, A. Galal, F. M. Abu-Attia and S. M. Azab, Carbon paste gold nanoparticles sensor for the selective determination of dopamine in buffered solutions, *J. Electrochem. Soc.*, 2010, **157**(9), F116–F123.
 - 40 R. N. Goyal, V. K. Gupta, M. Oyama and N. Bachheti, Gold nanoparticles modified indium tin oxide electrode for the simultaneous determination of dopamine and serotonin: application in pharmaceutical formulations and biological fluids, *Talanta*, 2007, **72**, 976–983.
 - 41 G.-Z. Hu, D.-P. Zhang, W.-L. Wu and Z.-S. Yang, Selective determination of dopamine in the presence of high concentration of ascorbic acid using nano-Au self-assembly glassy carbon electrode, *Colloids Surf., B*, 2008, **62**, 199–205.
 - 42 J. Li and X. Lin, Simultaneous determination of dopamine and serotonin on gold nanocluster/overoxidized-polypyrrole composite modified glassy carbon electrode, *Sens. Actuators, B*, 2007, **124**, 486–493.
 - 43 R. N. Goyal, A. Aliumar and M. Oyama, Comparison of spherical nanogold particles and nanogold plates for the oxidation of dopamine and ascorbic acid, *J. Electroanal. Chem.*, 2009, **631**, 58–61.
 - 44 N. F. Atta, A. Galal and R. A. Ahmed, Poly(3,4-ethylenedioxythiophene) electrode for the selective determination of dopamine in presence of sodium dodecyl sulfate, *Bioelectrochemistry*, 2011, **80**, 132–141.
 - 45 N. F. Atta, A. Galal and R. A. Ahmed, Direct and simple electrochemical determination of morphine at PEDOT modified Pt electrode, *Electroanalysis*, 2011, **23**, 737–746.
 - 46 N. F. Atta, A. Galal, F. M. Abu-Attia and S. M. Azab, Characterization and electrochemical investigations of micellar/drug interactions, *Electrochim. Acta*, 2011, **56**, 2510–2517.
 - 47 N. F. Atta, S. A. Darwish, S. E. Khalil and A. Galal, Effect of surfactants on the voltammetric response and determination of an antihypertensive drug, *Talanta*, 2007, **72**, 1438–1445.
 - 48 C. Li, Y. Ya and G. Zhan, Electrochemical investigation of tryptophan at gold nanoparticles modified electrode in the presence of sodium dodecylbenzene sulfonate, *Colloids Surf., B*, 2010, **76**, 340–345.
 - 49 G. A. Angeles, S. C. Avendaño, M. P. Pardavé, A. R. Hernández, M. R. Romo and M. T. R. Silva, Selective electrochemical determination of dopamine in the presence of ascorbic acid using sodium dodecyl sulfate micelles as masking agent, *Electrochim. Acta*, 2008, **53**, 3013–3020.
 - 50 J. Zheng and X. Zhou, Sodium dodecyl sulfate-modified carbon paste electrodes for selective determination of dopamine in the presence of ascorbic acid, *Bioelectrochemistry*, 2007, **70**, 408–415.
 - 51 S.-f. Liu, X.-h. Li, Y.-c. Li, Y.-f. Li, J.-r. Li and L. Jiang, The influence of gold nanoparticle modified electrode on the structure of mercaptopropionic acid self-assembly monolayer, *Electrochim. Acta*, 2005, **51**, 427–431.